



Supramolecular self-assembly of new thiourea derivatives directed by intermolecular hydrogen bonds and weak interactions: crystal structures and Hirshfeld surface analysis

Ilkay Gumus, et al. [full author details at the end of the article]

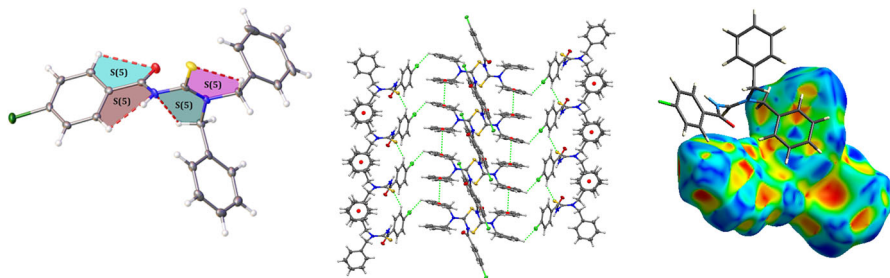
Received: 19 June 2018 / Accepted: 10 September 2018 / Published online: 18 September 2018
© Springer Nature B.V. 2018

Abstract

We synthesized and characterized a series of four closely related thiourea derivatives (**1–4**) obtained by reaction of 4-*R*-benzoyl chloride (R: H, Cl, CH₃, and OCH₃) with equimolar amount of potassium thiocyanate and dibenzylamine in dry acetone. The crystalline and molecular structures of the synthesized compounds **1–4** were examined to understand how the crystal packing of each compound altered when substituted by different functional groups at *para* position on the aromatic ring. Single-crystal X-ray diffraction analysis revealed that molecules of the prepared compounds assembled into supramolecular units connected via networks of similar intermolecular interactions. The packing arrangement of the compounds, however, was found to be different. We also conducted Hirshfeld surface analysis for all the synthesized compounds and followed the changes of different properties on these surfaces related to systematic variations of the substituent. Hirshfeld surface analysis and decomposed fingerprint plots showed that the structures were stabilized by H···H, H···S, O···H, N···H, C–H···π, and π···π intermolecular interactions, which contribute mostly to the packing of the species in the crystal. The two largest contributions to the packing of the molecules in the crystals were provided by H···H (51.6, 39.5, 54.4, and 51.4 %) and C–H···π (27.4, 27.1, 24.6, and 28.8 %) intermolecular interactions.

Electronic supplementary material The online version of this article (<https://doi.org/10.1007/s11164-018-3596-5>) contains supplementary material, which is available to authorized users.

Graphical abstract

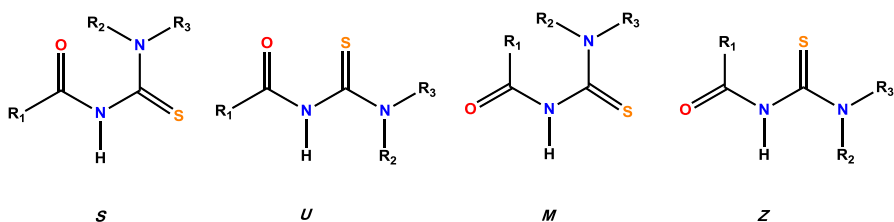


Keywords Thiourea derivatives · Hirshfeld surface analysis · Crystal structure · Supramolecular self-assembly · Noncovalent interactions

Introduction

Thiourea derivatives are known to be promising compounds in materials chemistry due to their ability to form intra- and intermolecular hydrogen bonds between NH donor groups and carbonyl oxygen/thiocarbonyl sulfur atoms [1–5]. The mutual effect between intra- and intermolecular hydrogen bonding strongly affects the chemical properties of these compounds. In addition, hydrogen bonds influence the conformational balance around the $-C(C=O)-N-(C=S)N-$ moiety core of thiourea derivative compounds. The four main forms of thiourea derivative compounds are *S*, *U*, *M*, and *Z*, relying on the formation of proper hydrogen bonds (Scheme 1). The feasibility of these compounds depends on the orientations adopted by the $C=O$ and $C=S$ double bonds with respect to the $C-N$ bonds (where *S*, *U*, *M*, and *Z* indicate the position of the $C=O$ and $C=S$ double bonds relative to the perpendicularly drawn $N-H$ bond) [6, 7].

Understanding of the conformational and structural properties of thiourea compounds has direct relevance to many applied fields such as heterocyclic synthesis intermediates, nonionic surfactants [8], organocatalysts [9–15], metal



Scheme 1 Plausible conformations of thiourea derivative compounds around the central $-C(O)NHC(S)N-$ moiety

coordination [26–30], and anion receptors [16–26]. In a recent study by Becker et al. [6, 27], 739 structures containing the $-\text{C}(\text{C}=\text{O})\text{N}(\text{C}=\text{S})\text{N}-$ moiety in the Cambridge Crystallographic Database were analyzed to determine the structural and conformational properties of these compounds. On the other hand, in another study on acyl thioureas, 440 crystal structures were found in the Cambridge Crystallographic Database and the majority (236 structures) displayed a characteristic intermolecular pattern forming dimers via $\text{N}-\text{H}\cdots\text{S}$ hydrogen bonding adopting an $R_2^2(8)$ motif [28, 29]. In addition, for better understanding of the contribution of structural and conformational properties to intermolecular interactions, Hirshfeld surfaces analysis of a few thiourea derivative compounds has been performed [30–34].

In this study, a series of functionalized thiourea derivative compounds with different functional groups (H, Cl, CH_3 , and OCH_3) at *para*-position on the aromatic ring were synthesized and characterized by Fourier-transform infrared (FT-IR) and ^1H and ^{13}C nuclear magnetic resonance (NMR) spectroscopy. Also, the crystal structure and conformational properties of synthesized compounds were determined via single-crystal X-ray diffraction studies. The corresponding crystalline packing of synthesized compounds is discussed on the basis of variable synthons, leading to formation of supramolecular structures, all of them essentially dictated by noncovalent interactions. Analysis of intermolecular contacts was performed based on the Hirshfeld surfaces and their associated two-dimensional (2D) fingerprint plots.

Experimental

Instrumentation

NMR spectra were recorded in dimethyl sulfoxide ($\text{DMSO}-d_6$) solvent on a Bruker Avance III 400 MHz NaNoBay FT-NMR spectrometer with tetramethylsilane as internal standard. Infrared spectra for each compound were recorded in the range of $400\text{--}4000\text{ cm}^{-1}$ on a PerkinElmer Spectrum 100 series FT-IR/FIR/NIR spectrophotometer Frontier ATR instrument.

X-ray single-crystal diffraction data were recorded on a Bruker APEX-II charge-coupled device (CCD) diffractometer. A suitable crystal was selected, coated with Paratone oil, and mounted onto a Nylon loop on a Bruker APEX-II CCD diffractometer. The crystal was kept at $T = 100\text{ K}$ during data collection. The data were collected with $\text{Mo K}\alpha$ ($\lambda = 0.71073\text{ \AA}$) radiation for compound **2** and **3** and $\text{Cu K}\alpha$ ($\lambda = 1.54178$) radiation for compound **1** and **4**, at crystal-to-detector separation of 40 mm. Using Olex2 [35], the structure was solved with the Superflip [36–38] structure solution program, using the Charge Flipping solution method and refined by full-matrix least-squares techniques on F^2 using ShelXL [39] with refinement of F^2 against all reflections. Hydrogen atoms were constrained by difference maps and were refined isotropically, and all nonhydrogen atoms were refined anisotropically. Molecular structure plots were prepared using PLATON [40].

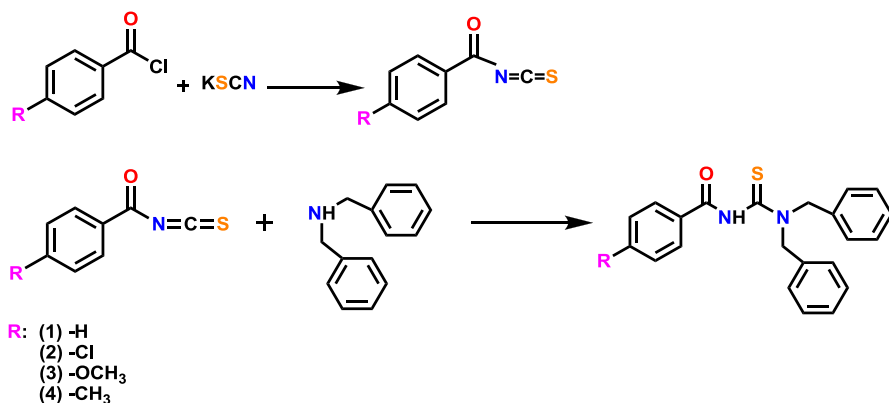
Hirshfeld surface analysis

Hirshfeld surface analysis and associated two-dimensional fingerprint plots of compounds **1–4** were calculated using CrystalExplorer 17 [41]. Hirshfeld surfaces were mapped with different properties, namely d_{norm} , shape index, and curvedness. d_{norm} is a normalized contact distance, defined in terms of d_e , d_i , and the van der Waals (vdW) radii of the atoms. The combination of d_e and d_i in the form of a 2D fingerprint plot provides a summary of intermolecular contacts in the crystal.

Synthesis of compounds **1–4**

Compounds **1–4** were prepared according to previously published methods [42–45]. Solution of aryl chloride (4-chlorobenzoyl chloride, 4-methylbenzoyl chloride, 4-methoxybenzoyl chloride, and benzoyl chloride) (5×10^{-2} mol) in dry acetone (50 mL) was added dropwise to suspension of potassium thiocyanate (5×10^{-2} mol) in acetone (30 mL). The reaction mixture was heated under reflux for 30 min, then cooled to room temperature. Solution of dibenzylamine (5×10^{-2} mol) in acetone (10 mL) was added, and the resulting mixture was stirred for 2 h. Thereafter, the reaction mixture was poured into hydrochloric acid (0.1 N, 300 mL), and the solution was filtered. The solid product was washed with water and purified by recrystallization from ethanol:dichloromethane mixture (1:1, *v:v*) (Scheme 2).

N-(Dibenzylcarbamothioyl)benzamide (1) Yield: 85 %. Color: White. Melting point: 418–420 K. FT-IR (ATR, ν , cm^{-1}): 3327, 3272 $\nu(\text{NH})$, 3030 $\nu(\text{Ar-CH})$, 1688 $\nu(\text{C=O})$, 1589 $\nu(\text{C=C})$, 748 $\nu(\text{C=S})$. ^1H NMR (400 MHz, DMSO- d_6 , δ , ppm): 10.99 (s, 1H, NH), 7.88 (d, 2H, $J = 8$ Hz, Ar-H), 7.60 (m, 1H, Ar-H), 7.49 (m, 4H, Ar-H), 7.41–7.32 (m, 6H, Ar-H), 7.21 (d, 2H, $J = 8$ Hz, Ar-H), 5.24 (s, 2H, CH_2), 4.69 (s, 2H, CH_2). ^{13}C NMR (100 MHz, DMSO- d_6 , δ , ppm): 183.46 (C=S), 164.51 (C=O), 135.79 (Ar-C), 135.07 (Ar-C), 132.75 (Ar-C), 132.41 (Ar-C), 128.72 (Ar-C), 128.48 (Ar-C), 128.39 (Ar-C), 128.25 (Ar-C), 127.81 (Ar-C), 127.35 (Ar-C), 55.56 (C-N), 54.68 (C-N).



Scheme 2 Synthesis of compounds **1–4**

4-Chloro-*N*-(dibenzylcarbamothioyl)benzamide (2) Yield: 80 %. Color: White. Melting point: 415–417 K. FT-IR (ATR, ν , cm^{-1}): 3267 $\nu(\text{NH})$, 3031 $\nu(\text{Ar-CH})$, 1687 $\nu(\text{C=O})$, 751 $\nu(\text{C=S})$, 751 $\nu(\text{C-Cl})$. ^1H NMR (400 MHz, $\text{DMSO-}d_6$, δ , ppm): 11.08 (s, 1H, NH), 7.88 (d, 2H, $J = 8$ Hz, Ar-H), 7.56 (d, 2H, $J = 8$ Hz, Ar-H), 7.49 (d, 2H, $J = 4$ Hz, Ar-H), 7.41–7.32 (m, 6H, Ar-H), 7.19 (d, 2H, $J = 8$ Hz, Ar-H), 5.25 (s, 2H, CH_2), 4.68 (s, 2H, CH_2). ^{13}C NMR (100 MHz, $\text{DMSO-}d_6$, δ , ppm): 183.16 (C=S), 163.54 (C=O), 137.29 (Ar-C), 135.80 (Ar-C), 135.03 (Ar-C), 131.56 (Ar-C), 130.19 (Ar-C), 128.72 (Ar-C), 128.48 (Ar-C), 127.81 (Ar-C), 127.40 (Ar-C), 55.66 (C-N), 54.72 (C-N).

***N*-(Dibenzylcarbamothioyl)-4-methoxybenzamide (3)** Yield: 84 %. Color: White. Melting point: 414–416 K. FT-IR (ATR, ν , cm^{-1}): 3188 $\nu(\text{NH})$, 3027 $\nu(\text{Ar-H})$, 1688 $\nu(\text{C=O})$, 752 $\nu(\text{C=S})$. ^1H NMR (400 MHz, $\text{DMSO-}d_6$, δ , ppm): 10.82 (s, 1H, NH), 7.91 (d, 2H, $J = 12$ Hz, Ar-H), 7.51 (d, 2H, $J = 8$ Hz, Ar-H), 7.39–7.32 (m, 6H, Ar-H), 7.20 (d, 2H, $J = 8$ Hz, Ar-H), 7.03 (d, 2H, $J = 12$ Hz, Ar-H), 5.25 (s, 2H, CH_2), 4.66 (s, 2H, CH_2), 3.83 (s, 3H, O- CH_3). ^{13}C NMR (100 MHz, $\text{DMSO-}d_6$, δ , ppm): 183.76 (C=S), 163.94 (C=O), 130.41 (Ar-C), 127.80 (Ar-C), 127.44 (Ar-C), 127.34 (Ar-C), 124.81 (Ar-C), 113.67, 55.48 (C-N), 54.66 (C-N), 40.19 (O- CH_3).

***N*-(Dibenzylcarbamothioyl)-4-methylbenzamide (4)** Yield: 88 %. Color: White. Melting point: 406–408 K. FT-IR (ATR, ν , cm^{-1}): 3365 $\nu(\text{NH})$, 3061, 3027 $\nu(\text{Ar-H})$, 1696 $\nu(\text{C=O})$, 747 $\nu(\text{C=S})$. ^1H NMR (400 MHz, $\text{DMSO-}d_6$, δ , ppm): 10.89 (s, 1H, NH), 7.80 (d, 2H, $J = 8$ Hz, Ar-H), 7.50 (d, 2H, $J = 8$ Hz, Ar-H), 7.39–7.28 (m, 8H, Ar-H), 7.19 (d, 2H, $J = 4$ Hz, Ar-H), 5.24 (s, 2H, CH_2), 4.66 (s, 2H, CH_2), 2.36 (s, 3H, CH_3). ^{13}C NMR (100 MHz, $\text{DMSO-}d_6$, δ , ppm): 183.58 (C=S), 164.39 (C=O), 142.63 (Ar-C), 135.82 (Ar-C), 135.09 (Ar-C), 129.95 (Ar-C), 128.93 (Ar-C), 128.71 (Ar-C), 128.46 (Ar-C), 128.33 (Ar-C), 127.80 (Ar-C), 127.42 (Ar-C), 55.57 (C-N), 54.67 (C-N), 21.03 (CH_3).

Results and discussion

Spectral characterization

Four benzamide derivative compounds were synthesized by reaction of 4-*R*-benzoyl chloride (*R*: H, Cl, CH_3 , and OCH_3) with equimolar amount of potassium thiocyanate and dibenzylamine in dry acetone. The products were isolated in high yield as pure colorless solid. The reaction pathways are given in Scheme 2.

The first evidence of the formation of the prepared compounds is given by the ^1H and ^{13}C NMR spectra of the compounds, in which typical signals belonging to -NH groups appear in the range of δ 10.87–11.01 ppm as singlet, and typical signals of C=S and C=O groups at around $\delta \approx 183$ and $\delta \approx 164$ ppm, respectively. In ^1H NMR spectra, aromatic proton signals were observed in the range of δ 7.91–7.02 ppm. Correlation spectroscopy (COSY) of obtained compounds, given as supplementary material, allowed unambiguous assignment of aromatic protons. In the ^1H NMR spectra of all compounds, interestingly, different ^1H resonances appeared for each of two $-\text{CH}_2-$ groups in $\text{DMSO-}d_6$ at δ 4.69 and 5.24 for

compound **1**, δ 5.25 and 4.68 ppm for compound **2**, δ 5.25 and 4.66 ppm for compound **3**, and δ 5.24 and 4.66 ppm for compound **4**. Since the resonance in the C(O)–NH–C(S)–N part gives a double-bond character to the single bond and slows the rotation of the C–N bond [3, 46–50], for all compounds, this restricted rotation results in formation of *E/Z* configurational isomerism in solution [3, 46–50]. Meanwhile, the ^{13}C NMR spectra of compounds **1–4** showed expected carbon signals. C–H carbon atoms were distinguished from quaternary carbon signals through heteronuclear multiple-quantum coherence (HMQC) spectra (see supporting information).

The $\nu(\text{C–H})$ stretching vibration mode for aromatic rings in compounds **1–4** appeared at 3324, 3266, 3188, and 3364 cm^{-1} , respectively. The $\nu(\text{C–H})$ stretching for alkyl groups ($-\text{CH}_2$) appeared in the region between 2900 and 3060 cm^{-1} for all compounds. The $\nu(\text{N–H})$ stretching modes of compounds **1** and **4** appeared at 3324 and 3364 cm^{-1} , close to the signals of free secondary amines (3400–3500 cm^{-1}). The $\nu(\text{N–H})$ stretching mode of compound **4** was shifted down to 40 cm^{-1} and broadened due to hydrogen-bond formation compared with compound **1** (Figs. 5S, 23S) [51]. The $\nu(\text{N–H})$ stretching modes of compounds **2** and **3** appeared at 3266 and 3188 cm^{-1} , respectively, lower than those in free secondary amines due to presence of intra- or intermolecular hydrogen bonds (Figures. 11S, 17S) [52]. The characteristic $\nu(\text{C=O})$ stretching modes for compounds **1–4** appeared at 1686, 1687, 1688, and 1696 cm^{-1} , respectively, lower than the free vibration mode of carbonyl group ($\sim 1720 \text{ cm}^{-1}$) [52]. This may be due to conjugative resonance and tautomerism effects in the amide-thioamide groups and the formation of possible intra- and intermolecular hydrogen bonds. The formation of possible C=S \cdots H–N/C intermolecular hydrogen bonds seems to strongly affect the frequency of the $\nu(\text{C=S})$ mode [53, 54]. It should be mentioned that, for the main thiourea molecule, this mode emerged at $\sim 1090 \text{ cm}^{-1}$ in the FT-IR spectrum, while higher values up to 1325 cm^{-1} have also been reported [55–57]. This difference results from mixed vibrations and strong vibrational coupling in thiocarbonyl derivatives containing nitrogen [58]. In the FT-IR spectra of compounds **1–4**, medium-intensity IR absorptions observed at around $\sim 750 \text{ cm}^{-1}$ are tentatively assigned to the $\nu(\text{C=S})$ mode. These values are in agreement with previous studies of the mentioned derivatives [59–61].

Crystal structure description

The crystalline and molecular structures of the synthesized compounds **1–4** were examined to understand how the crystal packing of each compound altered when different functional groups were substituted at *para* position on the aromatic ring. The molecular structure of the compounds **1–4**, with their atom numbering scheme, is shown in Fig. 1. The crystallographic data of the compounds are summarized in Table 1, while selected bond lengths and angles are gathered in Table 2.

The obtained thiourea derivative compounds **1–4** crystallize in the monoclinic $P112_1$ with $Z = 4$, monoclinic $C2/c$ with $Z = 8$, monoclinic $P2_1$ with $Z = 4$, and triclinic $P-1$ with $Z = 4$, respectively (Table 1). The unit cell parameters of all compounds were significantly different, indicating the role of the substituent in their

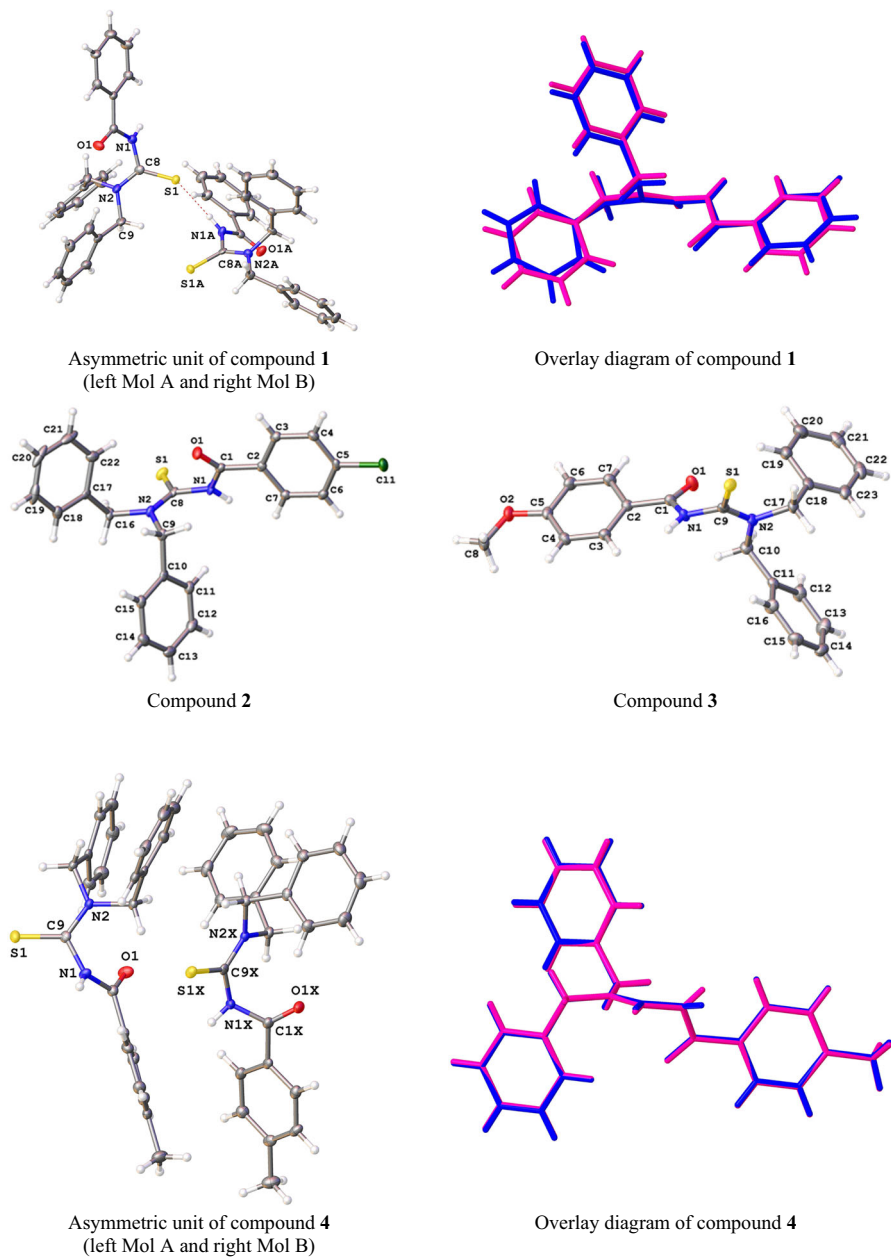


Fig. 1 Molecular structure of compounds 1–4, showing atom numbering (in both overlay diagrams, pink and blue represent Mol A and Mol B for compound 1 and 4, respectively)

Table 1 Crystal data and details of structure refinement for compounds 1–4

Parameter/compound	1	2	3	4
Empirical formula	C ₂₂ H ₂₀ N ₂ O ₅ S	C ₂₂ H ₁₉ ClN ₂ O ₅ S	C ₂₃ H ₂₂ N ₂ O ₅ S	C ₂₃ H ₂₂ N ₂ O ₅ S
Formula weight	360.46	394.90	390.48	374.48
Temperature (K)	293(2)	100.0	100.82	101.97
Crystal system	Monoclinic	Monoclinic	Monoclinic	Triclinic
Space group	<i>P112₁</i>	<i>P2₁/h</i>	<i>C2/c</i>	<i>P-1</i>
<i>a</i> (Å)	7.7262(2)	12.8325(5)	16.5220(5)	8.9420(4)
<i>b</i> (Å)	9.8674(3)	7.3045(4)	12.3275(4)	10.8916(5)
<i>c</i> (Å)	24.3538(7)	21.9267(11)	19.9111(6)	20.4173(9)
α (°)	90	90	90	82.170(2)
β (°)	90	106.067(2)	91.021(2)	78.859(2)
γ (°)	90	90	90	89.744(2)
Volume (Å ³)	1856.67(9)	1975.02(17)	4054.7(2)	1932.34(15)
<i>Z</i>	4	4	8	4
ρ_{calc} (g/cm ³)	1.290	1.328	1.279	1.287
μ (mm ⁻¹)	1.640	0.313	0.180	1.594
<i>F</i> (000)	760.0	824.0	1648.0	792.0
Crystal size (mm ³)	0.55 × 0.08 × 0.07	0.27 × 0.17 × 0.14	0.55 × 0.45 × 0.29	0.84 × 0.3 × 0.13
Radiation	Cu K α (λ = 1.54178 Å)	Mo K α (λ = 0.71073 Å)	Mo K α (λ = 0.71073 Å)	Cu K α (λ = 1.54178 Å)
2 θ range for data collection (°)	7.26–133.368	5.826–52.04	5.778–54.332	4.454–128.808
Index ranges	$-9 \leq h \leq 8$ $-11 \leq k \leq 11$ $-29 \leq l \leq 29$	$-15 \leq h \leq 15$ $-9 \leq k \leq 9$ $-27 \leq l \leq 27$	$-20 \leq h \leq 21$ $-15 \leq k \leq 15$ $-24 \leq l \leq 25$	$-10 \leq h \leq 9$ $-12 \leq k \leq 12$ $-23 \leq l \leq 23$

Table 1 continued

Parameter/compound	1	2	3	4
Reflections collected	19,479	55,676	23,515	42,432
Independent reflections	4673 [$R_{\text{int}} = 0.0578$, $R_{\text{sigma}} = 0.0595$]	3875 [$R_{\text{int}} = 0.0637$, $R_{\text{sigma}} = 0.0234$]	4476 [$R_{\text{int}} = 0.0408$, $R_{\text{sigma}} = 0.0320$]	6350 [$R_{\text{int}} = 0.0668$, $R_{\text{sigma}} = 0.0386$]
Data/restraints/parameters	4673/1/470	3875/0/244	4476/0/254	6350/0/489
Goodness of fit on F^2	0.816	1.084	1.039	1.077
Final R indexes [$I \geq 2\sigma(I)$]	$R_1 = 0.0374$, $wR_2 = 0.0888$	$R_1 = 0.0379$, $wR_2 = 0.0819$	$R_1 = 0.0425$, $wR_2 = 0.0944$	$R_1 = 0.0511$, $wR_2 = 0.1324$
Final R indexes [all data]	$R_1 = 0.0398$, $wR_2 = 0.0902$	$R_1 = 0.0494$, $wR_2 = 0.0870$	$R_1 = 0.0558$, $wR_2 = 0.1007$	$R_1 = 0.0567$, $wR_2 = 0.1365$
Largest diff. peak/hole ($e \text{ \AA}^{-3}$)	0.19/−0.19	0.45/−0.47	0.58/−0.52	0.45/−0.62

Table 2 Selected bond lengths (Å), and bond and torsion angles (°) of compounds **1–4**

Atoms	Length (Å)	Atoms	Angle (°)	Atoms	Angle (°)
Compound 1					
S1 C8	1.681(4)	C1 N1 C8	122.8(4)	C(8) N(1) C(1) O(1)	−11.4(6)
O1 C1	1.222(5)	C8 N2 C9	121.5(3)	C(8) N(1) C(1) C(2)	167.8(4)
N1 C1	1.376(5)	O1 C1 N1	121.3(4)	C(1) N(1) C(8) S(1)	−118.9(4)
N1 C8	1.407(6)	O1 C1 C2	122.6(4)	C(1) N(2) C(8) N(2)	61.6(6)
N2 C8	1.326(6)	N1 C8 S1	117.2(3)	C(9) N(2) C(8) S(1)	6.5(6)
N2 C9	1.474(6)	N2 C8 S1	125.9(3)	C(9) N(2) C(8) N(1)	−174.1(4)
N2 C16	1.485(5)	N2 C8 N1	116.9(4)	C(16) N(2) C(8) S(1)	−160.7(3)
Compound 2					
C11 C5	1.7419(17)	C1 N1 C8	123.23(14)	C(8) N(1) C(1) O(1)	4.3(3)
S1 C8	1.6844(17)	C8 N2 C9	124.21(14)	C(8) N(1) C(1) C(2)	−177.75(14)
O1 C1	1.221(2)	O1 C1 N1	122.41(16)	C(1) N(1) C(8) S(1)	114.52(16)
N1 C1	1.386(2)	O1 C1 C2	123.12(15)	C(1) N(1) C(8) N(2)	−66.8(2)
N1 C8	1.416(2)	N1 C1 C2	114.44(14)	C(9) N(2) C(8) S(1)	164.71(13)
N2 C8	1.330(2)	N1 C8 S1	118.27(12)	C(9) N(2) C(8) N(1)	−13.9(2)
N2 C9	1.483(2)	N2 C8 S1	125.44(13)	C(16) N(2) C(8) S(1)	−6.7(2)
N2 C16	1.473(2)	N2 C8 N1	116.28(14)	C(16) N(2) C(8) N(1)	174.67(14)
Compound 3					
S1 C9	1.6795(16)	O1 C1 N1	121.82(14)	C(8) O(2) C(5) C(4)	2.6(2)
O1 C1	1.2168(19)	O1 C1 C2	122.17(15)	C(8) O(2) C(5) C(6)	−177.14(14)
O2 C5	1.3629(18)	N1 C1 C2	116.01(13)	C(9) N(1) C(1) O(1)	6.7(2)
O2 C8	1.427(2)	C3 C2 C1	123.58(15)	C(9) N(1) C(1) C(2)	−172.29(13)
N1 C1	1.391(2)	C1 N1 C9	121.05(13)	C(1) N(1) C(9) S(1)	121.96(14)
N1 C9	1.4047(19)	C9 N2 C10	124.09(13)	C(1) N(1) C(9) N(2)	−58.9(2)
N2 C9	1.334(2)	N1 C9 S1	118.29(12)	C(10) N(2) C(9) S(1)	164.87(12)
N2 C10	1.479(2)	N2 C9 N1	116.91(14)	C(10) N(2) C(9) N(1)	−14.2(2)
Compound 4					
S1 C9	1.674(2)	C1 N1 C9	122.32(17)	C9 N1 C1 O1	10.0(3)
O1 C1	1.220(3)	C9 N2 C10	120.75(17)	C9 N1 C1 C2	−169.07(18)
N1 C1	1.388(3)	C9 N2 C17	124.31(17)	C1 N1 C9 S1	118.29(19)
N1 C9	1.417(3)	O1 C1 N1	122.28(19)	C1 N1 C9 N2	−62.9(3)
N2 C9	1.335(3)	O1 C1 C2	122.57(19)	C10 N2 C9 S1	−11.2(3)
N2 C10	1.472(3)	N1 C1 C2	115.14(17)	C10 N2 C9 N1	170.11(17)
N2 C17	1.480(3)	N1 C9 S1	118.30(15)	C17 N2 C9 S1	171.59(15)
C1 C2	1.496(3)	N2 C9 S1	125.33(16)	C17 N2 C9 N1	−7.1(3)

crystal packing. Compounds **2** and **3** contained one molecule in their asymmetric unit, while compounds **1** and **4** contained two molecules in their asymmetric unit, with these two different/independent molecules having slightly different bond lengths, bond angles, and dihedral angles. The atomic numbering scheme for all

compounds is given in Fig. 1, which also shows the contents of the asymmetric unit in each case. Overlay diagrams of compounds **1** and **4** are also given in Fig. 1.

The molecular structures of **1–4** consisted of similar thiourea cores $-\text{C}(\text{O})-\text{NH}-\text{C}(\text{S})-\text{N}<$ with different substitution groups. All synthesized compounds showed “S-shape” conformation (as defined in Scheme 1), in which the orientation between the $\text{C}=\text{O}$ and $\text{C}=\text{S}$ double bonds is opposite. The conformation around the amidic group in all compounds was near *cis* due to $\text{O}=\text{C}-\text{N}-\text{C}$, with torsion angles in the range between $-11.4(6)^\circ$ and $10.01(3)^\circ$, similar to those reported for related thiourea species [6, 62–65]. The amide and thioamide moieties ($\text{O}=\text{C}-\text{N}_1-\text{C}$ and $\text{C}-\text{N}_1-\text{C}=\text{S}$) torsion angles were $-11.4(6)^\circ$ and $-174.1(4)^\circ$ for compound **1**, $4.3(3)^\circ$ and $114.52(16)^\circ$ for compound **2**, $6.7(2)^\circ$ and $121.96(14)^\circ$ for compound **3**, and $10.01(3)^\circ$ and $118.29(19)^\circ$ for compound **4**. The dihedral angles between the planes defined by the amide and thioamide moieties of compounds **1–4** were 55.18° ($\text{O}_1-\text{C}_2-\text{N}_1$ and $\text{S}_1-\text{C}_1-\text{N}_1$), 63.15° ($\text{O}_1-\text{C}_1-\text{N}_1$ and $\text{S}_1-\text{C}_2-\text{N}_1$), 54.73° ($\text{O}_1-\text{C}_1-\text{N}_1$ and $\text{S}_1-\text{C}_2-\text{N}_1$), and 56.01° ($\text{O}_1-\text{C}_1-\text{N}_1$ and $\text{S}_1-\text{C}_2-\text{N}_1$), respectively. There was a significant deviation in the plane angle of compound **2** compared with the other derivatives (**1**, **3**, and **4**). This deviation occurs due to the chloro substituent. The dibenzyl substituents were twisted to the C_3N plane with torsion angles of -106.65° and -132.46° for compound **1** (Mol A), $-98.24(2)^\circ$ and -113.36° for compound **2**, -118.56° and -123.19° for compound **3**, and -108.99° and -126.35° for compound **4** (Mol A). In compounds **1–4**, phenyl rings of the dibenzyl part were essentially planar. In compounds **1**, **3**, and **4**, they were twisted with respect to each other by dihedral angle of 24.58° , 21.00° , and 13.25° , respectively. However, in compound **2**, phenyl rings of the dibenzyl part were parallel to each other with dihedral angle of 0° . The dihedral angle between the two planes defined by the phenyl ring of the benzamide part and the thioamide moiety was 51.38° , 72.45° , 63.07° , and 85.47° for the four compounds **1–4**, respectively. Considering the interplanar angles, it can be seen that they were very different from each other. The substituent at *para* position of the phenyl ring and the type of intermolecular hydrogen bonds in compounds **1–4** represent possible reasons for these differences.

The bond lengths and angles were similar for all compounds. The $\text{C}=\text{S}$ bond length for each compound was $1.681(4)$, $1.684(17)$, $1.679(16)$, and $1.674(2)$ Å, respectively, lying in the range for typical double bonds of $\text{C}=\text{S}$ groups [44, 45]. Also, the $\text{C}=\text{O}$ bond length for compounds **1–4** was $1.222(5)$, $1.221(2)$, $1.217(19)$, and $1.220(3)$ Å, respectively. In compounds **1–4**, the shortest $\text{C}-\text{N}$ bond length corresponded to C_8-N_2 [$1.326(6)$ Å], C_8-N_2 [$1.330(2)$ Å], C_9-N_2 [$1.334(2)$ Å], and C_9-N_2 [$1.334(2)$ Å], respectively, followed by C_1-N_1 [$1.376(5)$ Å], C_1-N_1 [$1.386(2)$ Å], C_1-N_1 [$1.391(2)$ Å], and $\text{C}_{11}-\text{N}_1$ [$1.388(3)$ Å]. The significant differences between these bond lengths suggest strong π -donation from N_2 , resulting in increased electron density in both carbon and sulfur atoms of the thioamide part [46]. The observed $\text{C}=\text{S}$ and $\text{C}=\text{O}$ double bonds, as well as the shortened $\text{C}-\text{N}$ bond lengths in the central $-\text{C}(\text{O})-\text{NH}-\text{C}(\text{S})-\text{N}<$ fragment, are typical for related thiourea compounds. The other main bond lengths of compounds **1–4** lie within the ranges obtained for similar compounds [34, 42–45, 66].

The crystal structure of the compounds is stabilized by intramolecular hydrogen bonds of type $\text{C}-\text{H}\cdots\text{N}$, $\text{C}-\text{H}\cdots\text{O}$, and $\text{C}-\text{H}\cdots\text{S}$. These intramolecular hydrogen

bonds cause formation of fused five-membered ring systems S(5) in each crystal structure (Fig. 2) and contribute to the conformation adopted in the solid. Intramolecular hydrogen bond parameters of all the compounds are listed in Table 3.

Despite the close similarity between compounds **1–4** in terms of their overall constitution and detailed molecular geometry, there were some significant differences in the nature of their supramolecular aggregation. The intermolecular hydrogen bonds, C–H \cdots π and $\pi\cdots\pi$ stacking interactions play an important role in the formation of three-dimensional (3D) supramolecular networks of compounds (Tables 3, 4 and 5). In the crystalline structure of the compounds, the most basic intermolecular interactions are the C–H \cdots S or N–H \cdots S hydrogen bonds between the amide –NH or –CH₂ groups (a strong H-bond donor) and the thiocarbonyl sulfur atom (a strong H-bond acceptor) of a partner molecule. These C–H \cdots S and N–H \cdots S hydrogen bonds lead to formation of dimeric homo- or heterosynthons. The homosynthon results when identical hydrogen bonds form between donor and acceptor moieties of two adjacent molecules, whereas the heterosynthon forms when two distinct types of hydrogen bond form. In both synthons, the potential hydrogen-bond donor atom is attached to a relatively electronegative atom (nitrogen or carbon), which is in *cis* position to the acceptor atom (thiocarbonyl sulfur or carbonyl oxygen atom) (Fig. 3).

It is well known that, in thiourea derivative compounds, the C=S group acts as a hydrogen-bond acceptor [52–65]. The two molecules in the asymmetric unit of compound **1** are mainly held together by intermolecular N–H \cdots S and weak C–H \cdots S hydrogen-bonding interactions: the sulfur atoms of the thiocarbonyl groups are

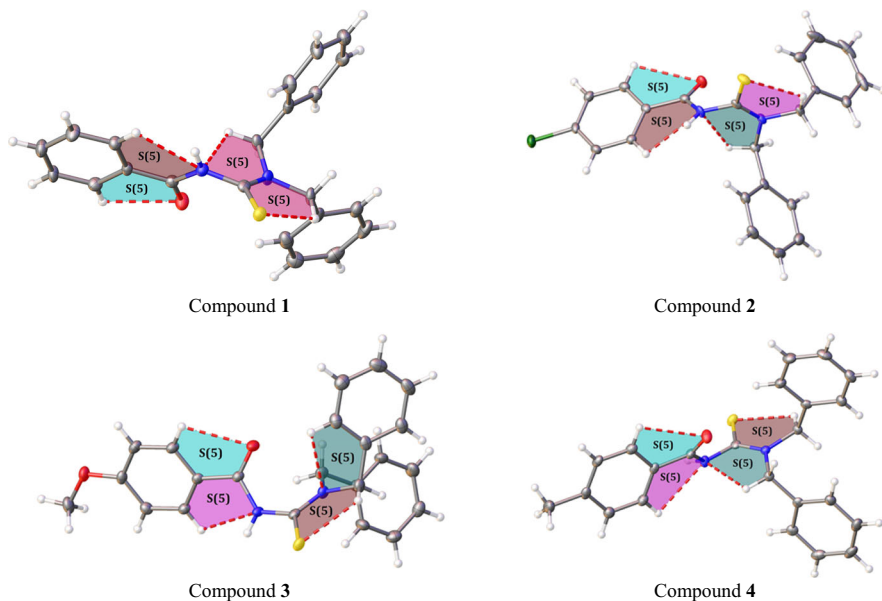


Fig. 2 Intramolecular hydrogen bonds cause formation of the fused S(5) ring motif in compounds **1–4**

Table 3 Intra- and intermolecular hydrogen bonds for compounds **1–4** (Å, °)

Compound	D–H···A	D(D–H)	D(H···A)	D(D···A)	∠(D–H···A)	Symmetry
1	N1–H1···S1A	0.86	2.54	3.332(3)	153	$-1 + x, y, z$
	N1A–H1A···S1	0.86	2.54	3.332(3)	153	x, y, z
	C9A–H9A···S1A	0.97	2.58	3.034(5)	109	–
	C6–H6···O1A	0.93	2.56	3.228(5)	129	$1 - x, 1 - y, -1/2 + z$
	C9–H9A···S1	0.97	2.58	3.087(5)	113	–
	C13A–H13A···O1	0.93	2.58	3.195(6)	124	$2 - x, 1 - y, 1/2 + z$
	C16–H16A···O1	0.97	2.60	2.995(5)	105	–
	C16–H16A···N1	0.97	2.35	2.797(6)	107	–
	C16A–H16C···N1A	0.97	2.38	2.815(6)	107	–
2	N1–H1···S1	0.88	2.56	3.4048(16)	161	$1 - x, 1 - y, 1 - z$
	C9–H9B···N1	0.99	2.39	2.807(2)	105	–
	C16–H16B···S1	0.99	2.54	3.0810(19)	114	–
3	N1–H1···S1	0.88	2.70	3.3513(13)	132	$1 - x, y, 3/2 - z$
	C10–H10B···N1	0.99	2.38	2.816(2)	106	–
	C12–H12···O1	0.95	2.29	3.229(2)	168	$1 - x, 1 - y, 1 - z$
4	C17–H17B···S1	0.99	2.53	3.0702(17)	114	–
	C4–H4···S1	0.95	2.86	3.779(2)	162	$2 - x, -y, 1 - z$
	C4X–H4X···S1X	0.95	2.87	3.785(2)	161	$1 - x, 1 - y, 1 - z$
	C10–H10B···S1	0.99	2.53	3.068(2)	114	–
	C10X–H10···S1X	0.99	2.53	3.071(2)	114	–
	C17–H17B···N1	0.99	2.35	2.803(3)	107	–
C17X–H17C···N1X	0.99	2.35	2.801(3)	107	–	

involved in the formation of the structure by hydrogen bonding. As shown in Fig. 4, intermolecular N–H···S (Table 3, 2.542 Å, symmetry code: $-1 + x, y, z$) and C–H···S (Table 3, 2.947 Å, symmetry code: $-1 + x, y, z$) hydrogen-bond interactions occur between the amide –NH group and the sulfur atom and between the amide –CH₂ and the sulfur atom, respectively. The combination of molecules generated through these N–H···S and weak C–H···S hydrogen-bonding interactions gives rise to the formation of dimeric $R_2^2(9)$ heterosynthons. The formation of these intermolecular C=S···H–N/C hydrogen bonds affects the $\nu(\text{C}=\text{S})$ stretching vibrations. In the FT-IR spectrum of compound **1**, the shift to lower frequency of the $\nu(\text{C}=\text{S})$ stretching vibration compared with the normal value is compatible with the formation of intermolecular hydrogen bonds [67, 68].

The formation of the mentioned dimers is also supported by the establishment of additional bifurcated C–H···O interactions (C6–H6···O1A, 2.56 Å, symmetry code: $1 - x, 1 - y, -1/2 + z$; C7–H7···O1A, 2.76 Å, symmetry code: $1 - x, 1 - y, 1/2 + z$) between the carbonyl oxygen atom and two hydrogen atoms of the phenyl ring (Fig. 4). In the FT-IR spectrum of the compound, the $\nu(\text{C}=\text{O})$ stretching vibration appears at 1688 cm^{-1} , confirming the presence of hydrogen-bonded carbonyl (vibration mode of carbonyl functional group is 1720 cm^{-1}). In addition,

Table 4 Geometrical parameters of C–H... π interactions for compounds **1–4** (\AA , $^\circ$)^{a,b}

C–H...Cg (J) ^c	H...Cg	H-perp ^d	\angle C–H...Cg	γ^e	C...Cg ^f
Compound 1					
C(11)–H(11A)...Cg(4) ⁱ	2.94	2.49	132	7.19	3.629(5)
Compound 2					
C(13)–H(13)...Cg(2) ⁱ	2.86	– 2.85	146	4.47	3.678(2)
C(14)–H(14A)...Cg(1) ⁱⁱ	2.99	2.97	148	6.23	3.827(2)
C(20)–H(20)...Cg(3) ⁱⁱⁱ	2.69	2.68	158	4.00	3.587(2)
Compound 3					
C(22)–H(22)...Cg(1) ⁱ	2.88	2.84	137	8.88	3.6336(19)
Compound 4					
C22–H22...Cg(5) ⁱ	2.87	2.78	143	14.32	3.673(3)
C22–H22X...Cg(2) ⁱⁱ	2.87	2.78	140	14.71	3.650(3)

^aSymmetry codes for compound **1**: $i = 1 + x, y, z$; for compound **2**: $i = 1/2 - x, 1/2 + y, 1/2 - z$; $ii = -1/2 + x, 3/2 - y, -1/2 + z$; $iii = 3/2 - x, -1/2 + y, 1/2 - z$; for compound **3**: $i = 1 - x, 1 - y, 1 - z$; for compound **4**: $i = x, y, z$; $ii = -1 + x, y, z$

^bCg(4) is the centroid of the rings C2A–C7A (Mol B) for compound **1**; Cg(1), Cg(2), and Cg(3) are the centroids of the rings C2–C7, C10–C15, and C17–C22 for compound **2**, respectively; Cg(1) is the centroid of the rings C2–C7 for compound **3**, and Cg(2) and Cg(5) are the centroids of the rings C11–C16 (Mol A) and C11X–C16X (Mol B) for compound **4**, respectively

^cCenter of gravity of ring J (plane number above)

^dPerpendicular distance of H to ring plane J

^eAngle between Cg–H vector and ring J normal

^fDistance between C-atom and the nearest carbon atom in the benzene ring

in the FT-IR spectrum, marker bands for C–H...O torsion mode representing a typical C–H...O hydrogen bond appeared at about 1490 and 1418 cm^{-1} (Fig. 6S) [69].

In compound **2**, the presence of the electron-donating chlorine atom, at *para* position on the phenyl ring of benzamide part, had a greater influence on the molecular packing compared with in compound **1**. In compound **2**, a series of dimerization occurs through formation of the consecutive $R_2^2(8)$, $R_2^2(12)$, $R_2^2(14)$, and $R_2^2(28)$ synthons. The N–H...S hydrogen bond, occurring between thiocarbonyl sulfur atom and amide hydrogen atom, leads to thioamide $R_2^2(8)$ homosynthon, while the C–H...S hydrogen bond, occurring between thiocarbonyl sulfur atom and aromatic ring hydrogen atom, leads to $R_2^2(14)$ homosynthon. The C–H...S hydrogen bond, which shares the same sulfur atom of the previous interaction, reinforces the strength/cohesion between dimers. However, the establishment of an additional interaction, the C–H...O between the aromatic ring hydrogen atom and the carbonyl oxygen atom, leads to $R_2^2(12)$ homosynthon chains along *b*-direction. Finally, the chlorine substituent in compound **2** establishes hydrogen- and halogen-bonding interactions, and a larger ring $R_2^2(28)$ homosynthon occurs via C–H...Cl interactions, in which the aromatic-ring carbon atom acts as a donor to the chloro atom of the

Table 5 Geometrical parameters of $\pi\cdots\pi$ interactions for compound **2** (Å, °)

Rings I–J ^a	Cg(I)⋯Cg(J) ^b	γ^c	Cg(I)-perp ^d	Cg(J)-perp ^e
Compound 1 ^f				
–	–	–	–	–
Compound 2				
Cg(2)⋯Cg(3) ⁱ	3.7783(12)	27.2	–3.3602(8)	3.4913(8)
Cg(3)⋯Cg(2) ⁱⁱ	3.7782(12)	22.5	3.4913(8)	–3.3602(8)
Compound 3 ^f				
–	–	–	–	–
Compound 4 ^f				
–	–	–	–	–

^aCg(1) and Cg(2) are the centroids of rings C2–C7 and C10–C15 for compound **2**, respectively

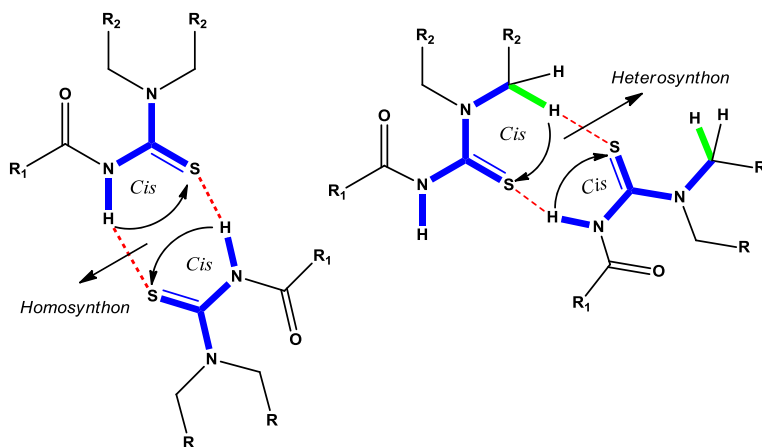
^bCentroid distance between ring I and ring J

^cAngle between the centroid vector Cg(I)⋯Cg(J) and the normal to plane J

^dPerpendicular distance of Cg(I) on ring J (Å)

^ePerpendicular distance of Cg(J) on ring I (Å)

^fInteractions greater than 4 Å. Symmetry codes for compound **2**:
i = *x*, 1 + *y*, *z*; *ii* = *x*, –1 + *y*, *z*

**Fig. 3** Formation of homosynthon and heterosynthon in the compounds

partner molecule (Fig. 5). The deformation bands revealed in the FT-IR spectrum can also be used as marker bands of the C–H⋯O dimer. To recognize the dimer of a C–H⋯O = C hydrogen bond, a characteristic split bending absorption was detected for the C–H⋯O=C hydrogen bond in the range of 1475–1425 cm^{-1} corresponding to torsional $\tau\text{C–H}\cdots\text{O}$ deformation of the mentioned dimer [69].

Compound **2** is also stacked in parallel fashion, forming a layered 3D structure held together by $\pi\cdots\pi$ intermolecular interactions with plane separation of 3.778 Å

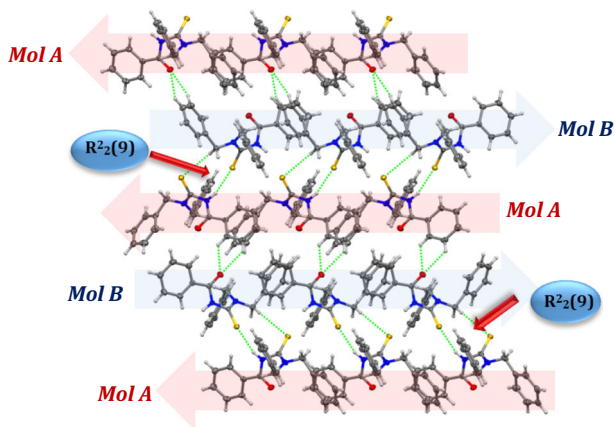


Fig. 4 Supramolecular framework in compound **1** generated via N–H...S, C–H...S, and C–H...O interactions

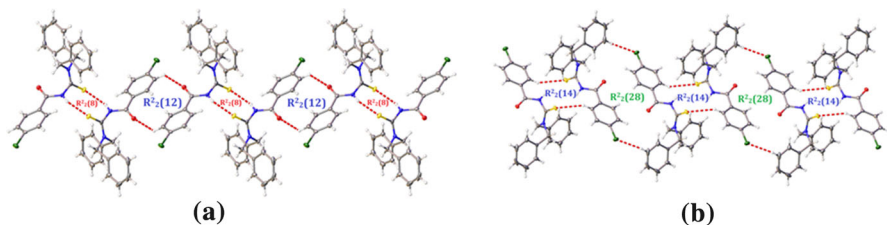


Fig. 5 **a** Consecutive formation of $R_2^2(8)$ and $R_2^2(12)$ synthon generated through C–H...S and C–H...O hydrogen bonds, **b** consecutive formation of $R_2^2(14)$ and $R_2^2(28)$ synthon generated via C–H...S and C–H...Cl hydrogen bonds of compound **2**, respectively

and symmetry code $x, 1 + y, z$ (Fig. 6a). These supramolecular layers were also expanded by C–H...Cl interactions (Fig. 6b). Thus, the 3D supramolecular structure of compound **2** is generated due to a mixed combination of these intermolecular interactions, which include slipped $\pi \cdots \pi$ stacking between aromatic rings of adjacent molecules. The main difference is that, in compound **2** compared with compound **1**, face-to-face $\pi \cdots \pi$ stacking interactions are formed, influencing the final solid-state architecture of the compound. In addition, in the structure, the molecules associate along b axis through $\pi \cdots \pi$ interactions to construct a helical chain motif (Fig. 6c).

In compound **3**, the N–H...S interaction occurs between the N–H group and the thiocarbonyl sulfur atom of a neighboring molecule. This leads to the formation of a dimer, which is obtained through a $R_2^2(8)$ homosynthon (Fig. 7). The position of the methoxy group in compound **3** plays an important role in the design of the supramolecular network of the compound. The substitution of methoxy group at *para* position on the phenyl ring of benzamide part leads to intermolecular C–H...O interactions. This interaction occurs between a methoxy group oxygen atom and a phenyl ring hydrogen atom, leading to the formation of $R_2^2(28)$ synthon. In the

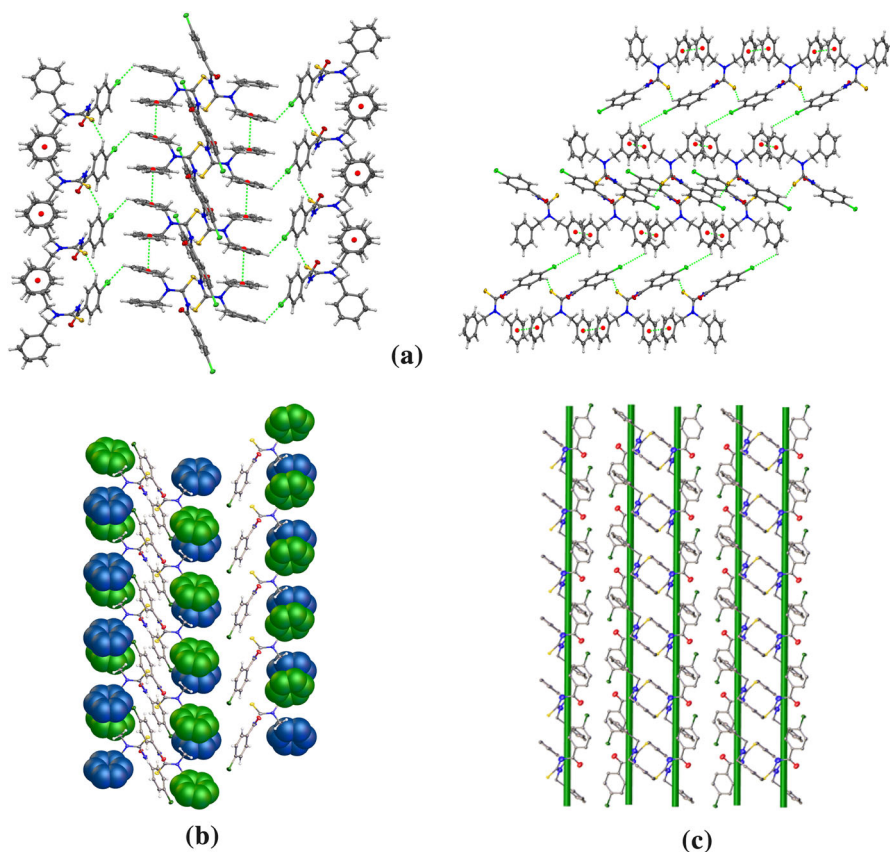


Fig. 6 **a** Molecules of compound **2** link one another by self-complementary C–H...S and C–H...Cl hydrogen bonds and π ... π stacking interactions, leading to formation of a layered assembly, **b** the face-to-face π ... π interactions shown in space-filling representation, **c** the helical chain formed along *b* direction

crystalline structure of compound **3**, other intermolecular interactions are the C–H...O (C12–H12...O1, 2.296 Å, symmetry code: $1 - x, 1 - y, 1 - z$) hydrogen-bond interaction between the carbonyl group oxygen atom and the phenyl ring hydrogen atom of a neighboring molecule and the C–H...S interaction between the thiocarbonyl sulfur atom and the phenyl ring hydrogen atom of a vicinal molecule. The combination of molecules generated through the C–H...O and C–H...S hydrogen-bonding interactions gives rise to the formation of consecutive dimeric $R_2^2(18)$ homosynthons (Fig. 8). These synthons are only found in compounds **2** and **3**. In the FT-IR spectrum, these C–H...O dimer interactions are also characterized by the appearance of a split of bending absorption bands in the range between 1425 and 1475 cm^{-1} [69].

In compound **3**, C–H... π stacking interaction occurs, in which the phenyl ring carbon atom in the molecule acts as a hydrogen-bond donor to the centroid of the phenyl ring in the neighboring molecule (C–H... π , 2.878 Å, symmetry code: $1 - x, 1 - y, 1 - z$), thus generating a one-dimensional polymeric chain aligned along the

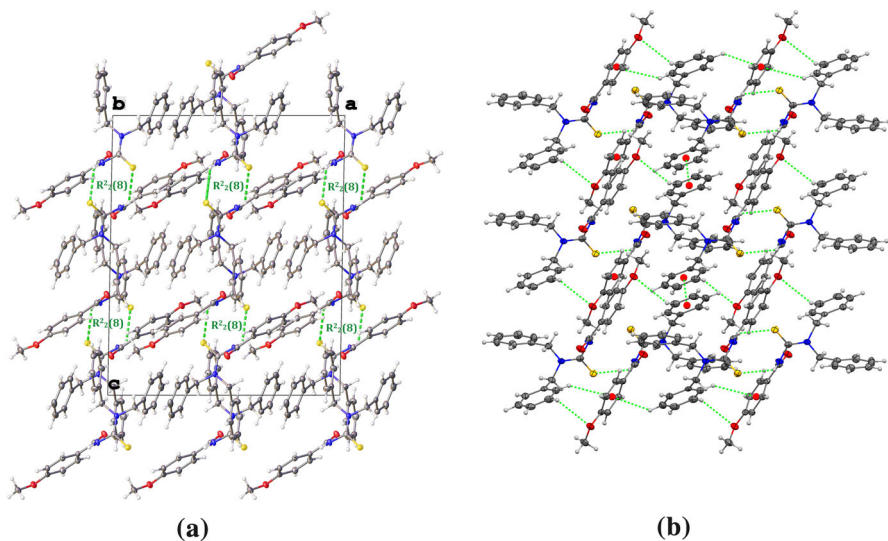


Fig. 7 **a** Supramolecular framework in compound **3** generated via C–H...O, C–H...S, and N–H...S hydrogen bonds, and C–H... π and π ... π stacking interactions along *b*-axis, **b** crystal packing of compound **3** along *c*-axis

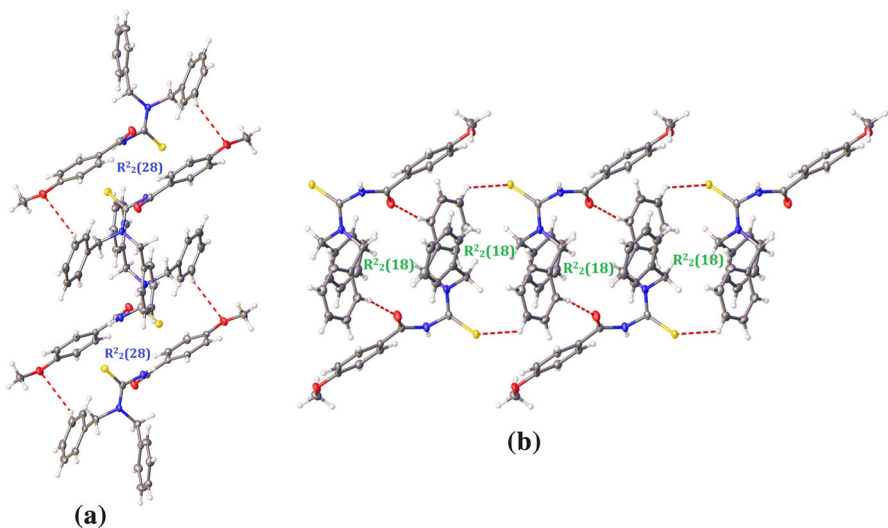


Fig. 8 **a** The formation of $R_2^2(28)$ homosynthon generated through C–H...O hydrogen bonds, **b** the formation of consecutive $R_2^2(18)$ homosynthon generated via C–H...S and C–H...O hydrogen bonds of compound **3**, respectively

b-axis (Fig. 7). In addition, the very weak parallel-displaced π ... π interaction (symmetry code: $3/2 - x, 1/2 - y, 1 - z$) between the dibenzylamine rings of two adjacent molecules is observed, forming a supramolecular layered assembly (Fig. 7).

The asymmetric unit of compound **4** consists of two independent molecules (Mol A and Mol B). In the asymmetric unit of compound **4**, the pairs of independent molecules are connected via weak N–H... π , C–H... π , and C–H...S interactions (Fig. 9). The N–H... π and C–H... π interactions occur between the amide NH group and the phenyl ring of the benzamide part and between the –CH₂/phenyl hydrogen atom and the phenyl ring of the benzamide part, respectively. In these interactions, the –CH₂/phenyl carbon atom in the molecule acts as a hydrogen-bond donor to the centroid of the phenyl ring in the neighboring molecule. The C–H...S interaction occurs between the –CH₂ hydrogen atom and the thiocarbonyl sulfur atom.

In addition, there are C–H...O intramolecular hydrogen bonds in the crystal lattice of compound **4** (C8C–H8C...O1X, 2.626 Å, symmetry code: 2 – x, 1 – y, 1 – z; C8X–H8XA...O, 2.63 Å, symmetry code: 2 – x, –y, 1 – z). The carbonyl group oxygen atoms interact with the methyl group of the benzene ring of the following molecule. So, the molecules of compound **4** line up in head-to-tail zigzag form in the crystal through C–H...O interactions (Fig. 10).

Compounds **1** and **4** contain two independent molecules in the asymmetric unit, which prevents formation of dimeric motifs due to the unsuitable orientations between hydrogen-bond donor and acceptor groups of the molecules in the asymmetric unit. In compounds **1** and **4**, the angle between a plane through the thioamide moieties (C1–N1–C7=S1) of molecules in the asymmetric unit is 22.99° and 69.13°, respectively. The thioamide moiety is not flat in both compounds. Although the relative orientation of the interacting molecules is different, compounds **2** and **3** form dimer motifs with almost the same type of intermolecular interactions. The angle between a plane through the thioamide moieties (C1–N1–C7=S1) of adjacent molecules is 0° in compound **2**, but adopts a value of 86.64° in compound **3**. The angle between the plane of the benzamide phenyl ring of adjacent molecules is 0° in compound **2** but 32.78° in compound **3**. The phenyl rings of benzamide part of compound **2** are parallel to each other, whereas those of **3** are tilted at $\theta = 32.78^\circ$ relative to each other. The thioamide moiety is flat in compound **2** but not in compound **3**. It can be said that the different geometries of the dimeric synthons and types of interaction reveal a profound influence of the substituent for compounds **2** and **3**.

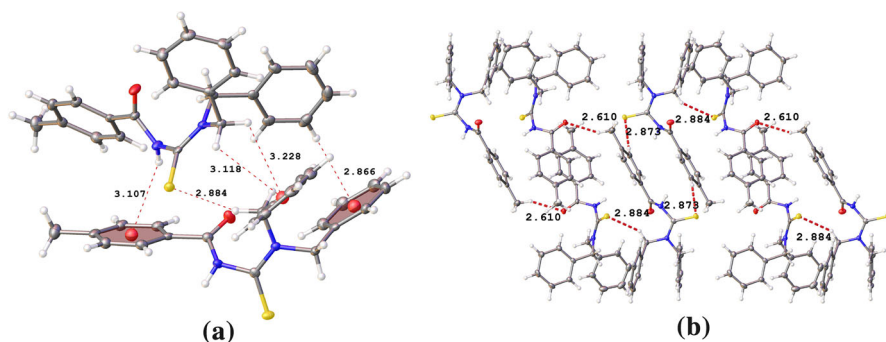


Fig. 9 **a** The intermolecular interactions between two molecules in the asymmetric unit of compound **4**, **b** the intermolecular interactions in crystal lattice

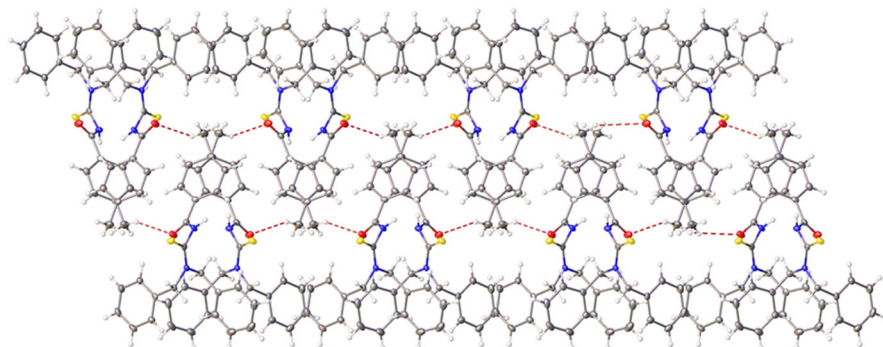


Fig. 10 The C–H...O interactions of compound **4**, leading to formation of a head-to-tail zigzag form in the crystal

The Cambridge Structural Database was searched for general *N*-dibenzylcarbamothioyl molecules with any substituents on the aromatic ring of benzamide part. Five structures were found, viz. 3-[[[(dibenzylcarbamothioyl)amino]carbonyl]benzamide (AGEDAT), 1,1-dibenzyl-3-(4-fluorobenzoyl)thiourea (AXABOR), 1,1-dibenzyl-3-(3-chlorobenzoyl)thiourea (EVEKIA), 3-benzoyl-1,1-dibenzylthiourea (KUZBUR), and 2-bromo-*N*-(dibenzylcarbamothioyl)benzamide (URENEL). AXABOR has $R_2^2(8)$, $R_2^2(14)$, and $R_2^2(12)$ homosynths generated via N–H...S, C–H...S, and C–H...O hydrogen bonds, respectively. They have the same synthon motifs as observed in compounds **2** and **3** in this study. EVEKIA forms $R_2^2(8)$ homosynths that are connected to each other via N–H...S interactions. KUZBUR is the same molecule as compound **1** synthesized in this work. Although they have similar N–H...S and C–H...O interactions, compound **1** has an additional heterosynthon generated via N–H...S and C–H...S. In addition, KUZBUR and compound **1** have similar bond lengths and angles, but different space groups. URENEL and AGEDAT are structurally very different from the compounds of this study and do not form synths.

Hirshfeld surface analysis

To provide further insight into the crystal packing of compounds **1–4**, a complete definition of the intermolecular interactions was obtained using Hirshfeld surface analysis. Figure 11 shows surfaces mapped over the d_{norm} property, in a similar orientation of front and back surfaces. The Hirshfeld surfaces of all compounds mapped with the d_{norm} are shown as transparent to allow visualization of the molecules. Red, blue, and white regions show distances shorter or longer than van der Waals radii and equal to the sum of the van der Waals radii, respectively [70, 71]. The Hirshfeld surfaces mapped with the d_{norm} function of compounds **1–4** reveal several red areas indicating close contacts between atoms on the surface (Fig. 11). The effect of different substituent groups at *para* position is clearly illustrated.

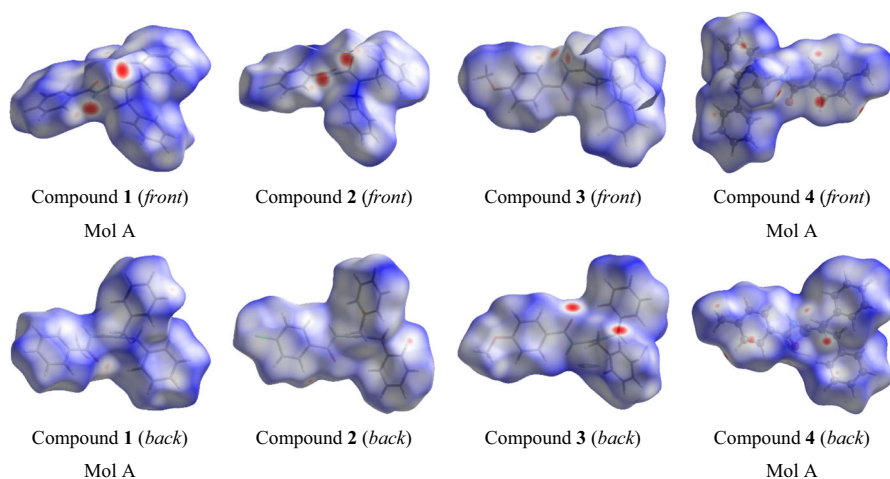


Fig. 11 Views of Hirshfeld surfaces mapped with d_{norm} in two orientations as front and back view

On the Hirshfeld surface mapped with the d_{norm} function of compound **1**, the two largest red spots correspond to two hydrogen bonds formed between the thiocarbonyl sulfur atom and the hydrogen of the amide ($\text{N-H}\cdots\text{S}$). Additional slight red areas are in accordance with the $\text{C-H}\cdots\text{S}$ interaction bond between the thiocarbonyl sulfur atom and the aromatic ring hydrogen. The $\text{C-H}\cdots\text{O}$ contacts on the d_{norm} Hirshfeld surface are displayed from faint red to white, meaning that these contacts are nearly equal to the van der Waals separation. These intermolecular contacts in compound **1** are indicated by arrows in Fig. 12.

In the d_{norm} Hirshfeld surface of compound **2**, the two large red spots correspond to intermolecular $\text{N1-H1}\cdots\text{S1}$ interactions. These strong spots are characteristic for the cyclic hydrogen-bond dimer motif. One additional slight red area is in accordance with the $\text{C-H}\cdots\text{S}$ interaction bond between the thiocarbonyl sulfur atom

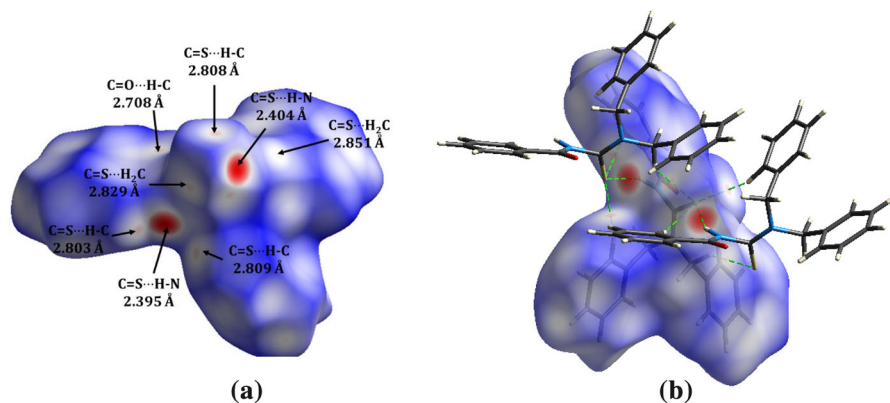


Fig. 12 **a** Hirshfeld surfaces of compound **1** mapped with d_{norm} function, **b** $\text{N-H}\cdots\text{S}$ and $\text{C-H}\cdots\text{S}$ hydrogen-bond interactions between the two parent molecules marked with dashed lines

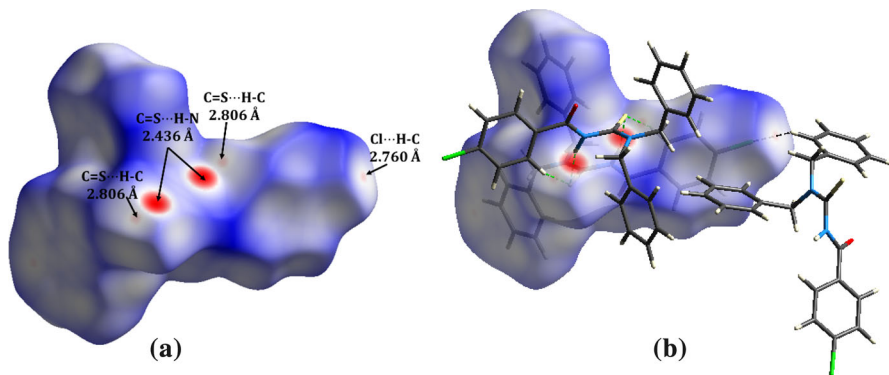


Fig. 13 **a** Hirshfeld surfaces of compound **2** mapped with d_{norm} function, **b** N–H...S, C–H...S, and C–H...Cl hydrogen-bond interactions between the two parent molecules marked with dashed lines

and the aromatic ring hydrogen (C–H...S). In compound **2**, an additional intramolecular C–H...Cl hydrogen bond is also observed as a weak red spot due to the presence of the chloro group at *para* position. The Hirshfeld surface mapped with the d_{norm} function and N–H...S, C–H...S, and C–H...Cl hydrogen-bond interactions between two parent molecules, marked with dashed lines for compound **2**, are shown in Fig. 13b.

In contrast to compounds **1** and **2**, in compound **3**, the two largest red spots correspond to C–H...O hydrogen-bond interactions, formed between the carbonyl oxygen atom and the hydrogen atom of the benzamide ring (C–H...O). It was observed that the presence of the methoxy group in compound **3** altered the intermolecular hydrogen bonds. Therefore, the arrangements of the molecules in the crystal packing are different from each other. As seen in Fig. 14a, two medium and two slight small red areas occurred due to stronger N–H...S and C–H...S interactions. The N–H...S and C–H...S interactions are weaker than C–H...O interactions.

In the Hirshfeld surface of compound **4** (Mol A), mapped with the d_{norm} function, a lot of medium red spots were revealed. Three of them correspond to C–H...S hydrogen bonds, as also observed in the other three compounds (**1–3**). The two small red spots are associated with C–H...O hydrogen-bonding interactions, occurring between the carbonyl oxygen atom and the methyl group hydrogen atom. Also, molecules of compound **4** were held together by π ... π stacking interactions occurring between aromatic rings of neighboring molecules, represented on the front and back surfaces as three small red spots (Fig. 15). The greatest difference between compound **4** and the other compounds is the lack of N–H...S interaction in compound **4**. However, in case of compound **4**, the presence of a methyl group increased the formation of additional weak C–H...S hydrogen bonds, represented on the Hirshfeld surface as two small red areas.

Hirshfeld surfaces mapped with the shape index and curvedness were used to assign characteristic packing modes and planar stacking arrangements of compounds **1–4**. On the Hirshfeld surface mapped with the shape index function for compound **2**, “bow-tie” patterns were noticed, which indicate the presence of aromatic stacking

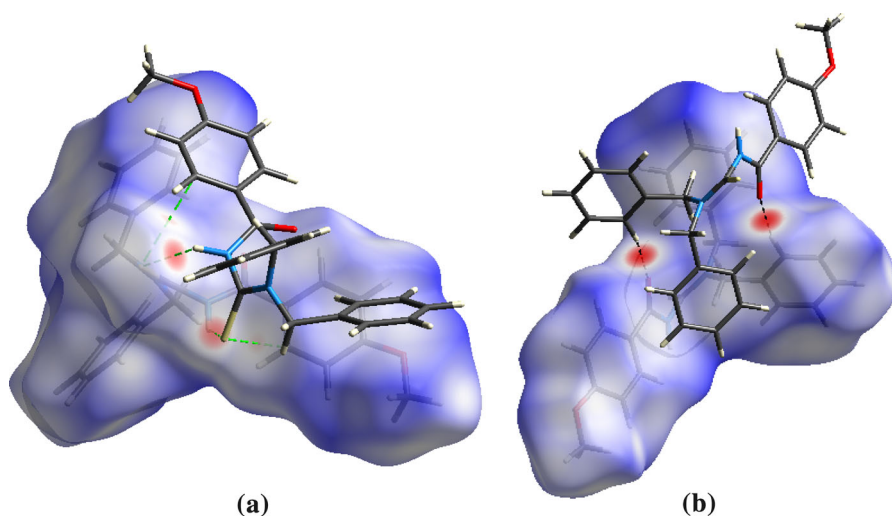


Fig. 14 **a** N–H...S and C–H...S, and **b** C–H...O hydrogen-bond interactions between the two parent molecules marked with dashed lines for compound **3**

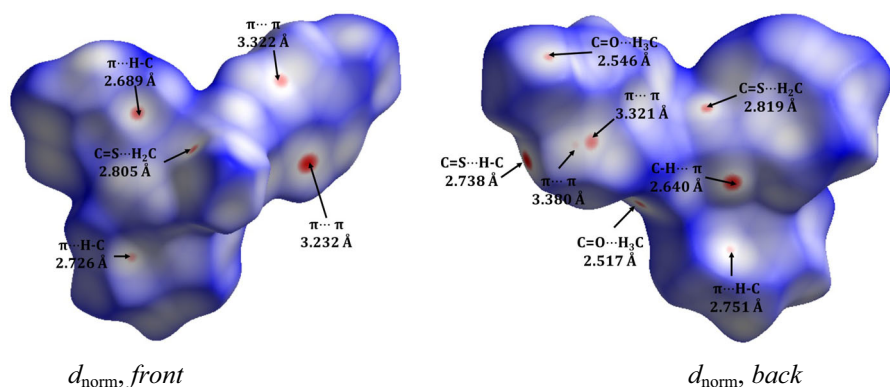


Fig. 15 Intermolecular interactions in the Hirshfeld surface mapped with d_{norm} for compound **4**

interactions (marked with circles in Fig. 16). The relatively large and green flat regions, drawn by circles on the coincident curvedness surfaces, provide proof for the existence of aromatic stacking interactions for compounds [72–79]. For compounds **1**, **3**, and **4**, the close aromatic stacking interactions were not as noticeable as for compound **2**, because there is no evidence of adjacent bow-tie patterns on the shape index surfaces. On the Hirshfeld surface mapped with the shape index function, nonreciprocal red and blue triangles, corresponding to C–H... π interactions (marked with circles in Fig. 17), were seen for compounds **1** and **3**.

The 2D decomposed fingerprint plots and relative contributions of various intermolecular interactions to the Hirshfeld surface area of compounds **1–4** are displayed in Fig. 18. Analysis of the decomposed fingerprint plots reveals that van der Waals forces (H...H contacts) play the most important role in the packing of the

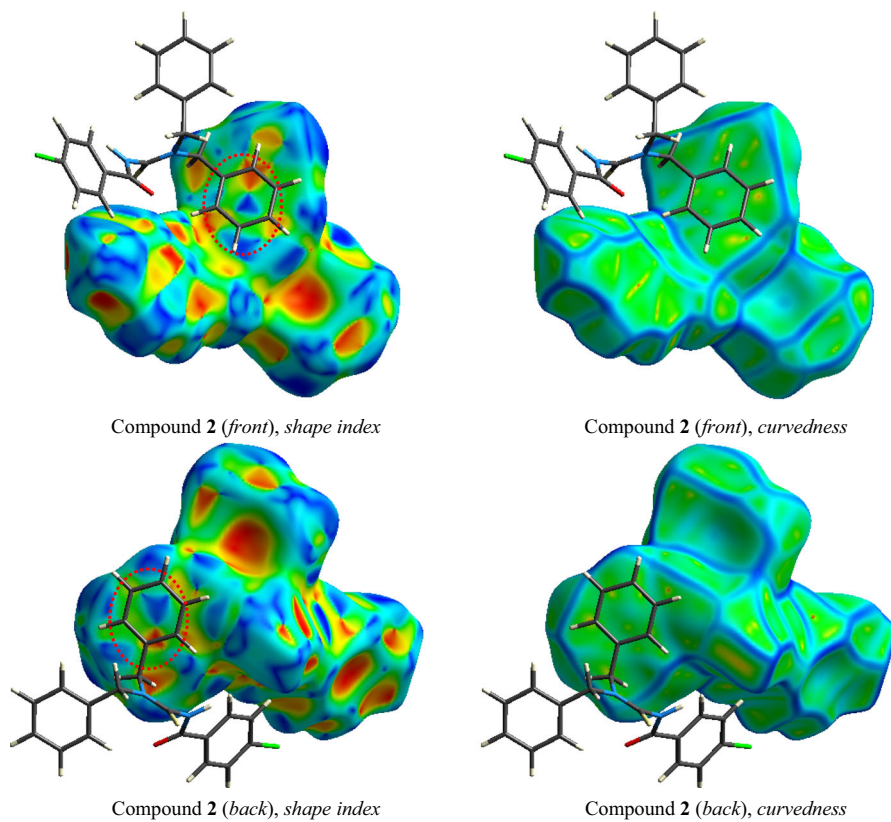


Fig. 16 Hirshfeld surfaces of compound 2 mapped with shape index and curvedness function. Areas marked with ovals represent $\pi\cdots\pi$ stacking interactions in shape index and flat regions in curvedness

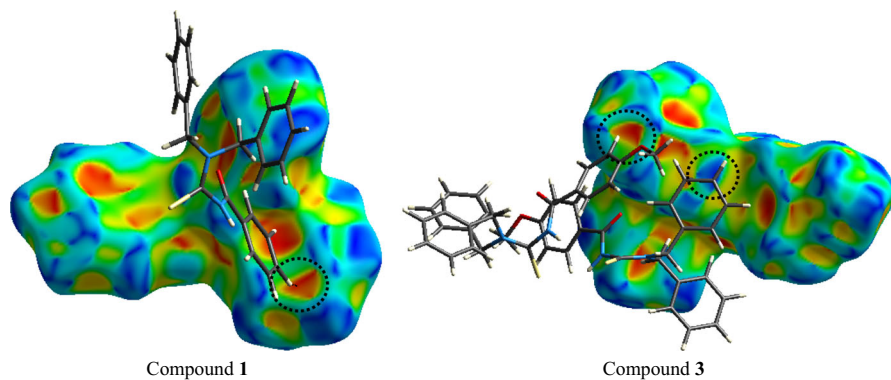


Fig. 17 C-H $\cdots\pi$ (orange triangles) and $\pi\cdots$ H-C (blue triangles) interactions on the Hirshfeld surfaces of compounds 1 and 3 mapped with shape index function

species in the structures. The H...H interactions in compounds 1–4 correspond to 51.6, 39.5, 54.4, and 51.4 % of the total Hirshfeld surfaces, respectively, being intensely visible in the middle of the two-dimensional fingerprint plot. Since the percentages of the surface H...H interactions in compound 1, 3, and 4 are very similar, it can be assumed that H...H contacts contribute almost equally to the packing in these compounds. However, in compound 2, the percentage of H...H interactions is decreased due to the substitution with the chlorine atom.

For compounds 1–4, the H...S intermolecular interactions in the 2D fingerprint plot represent N–H...S interactions, representing one of the closest contacts in the structures and viewed as red spots on the d_{norm} surface. The H...S intermolecular interactions are seen as a sharp spike in the 2D fingerprint plots, accounting for 12.1, 10.4, 8.4, and 11.7 % of the total Hirshfeld surfaces, respectively. It can be said that

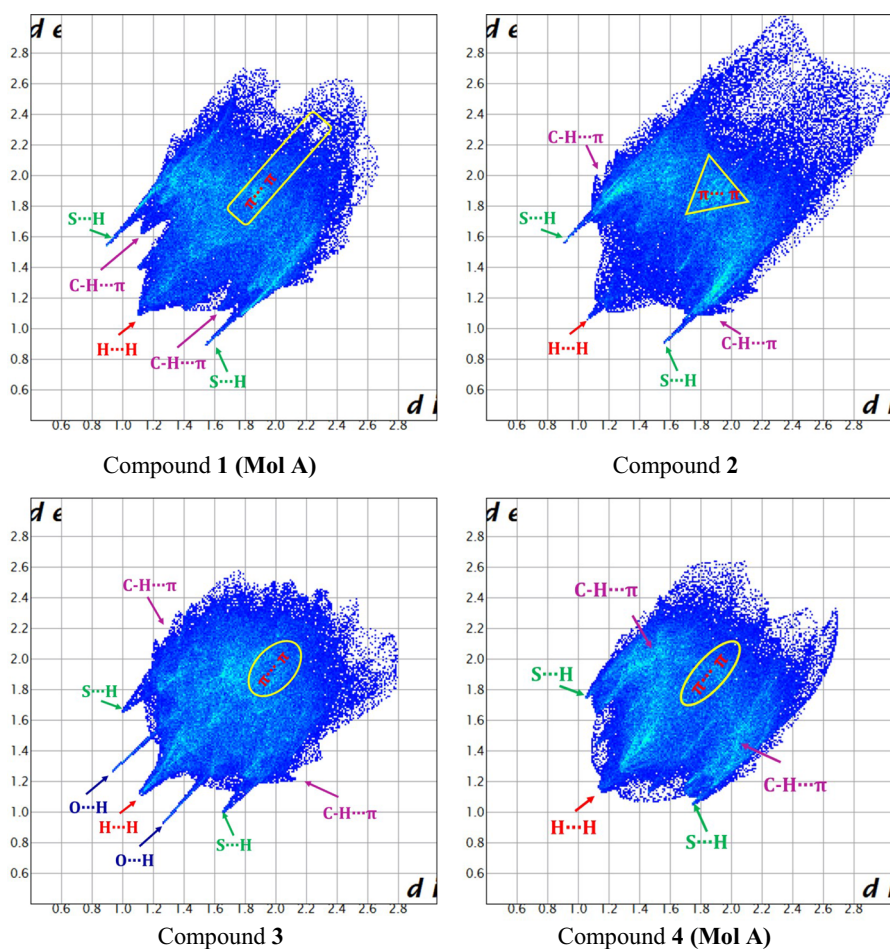


Fig. 18 Two-dimensional decomposed fingerprint plots and relative contributions of various intermolecular interactions to the Hirshfeld surface area of compounds 1–4

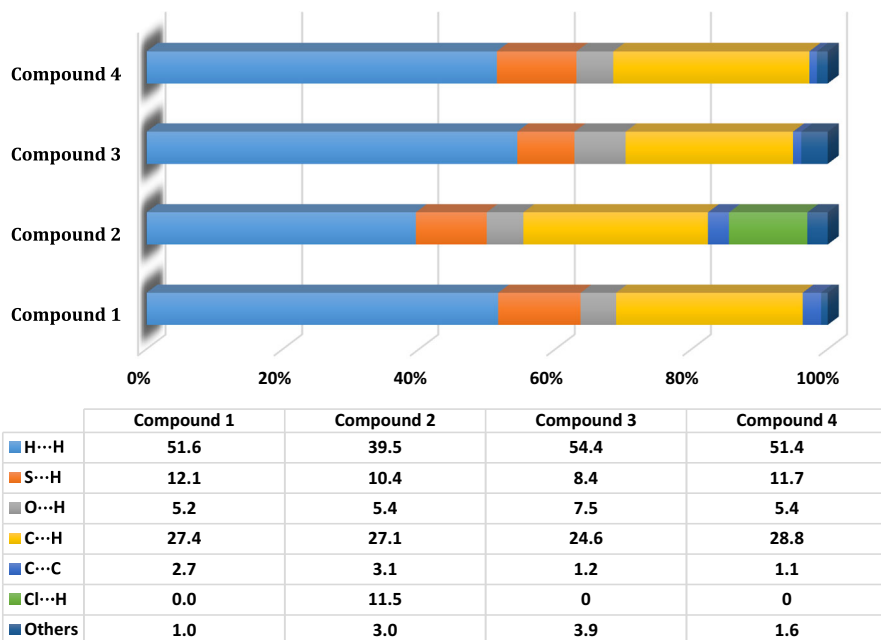


Fig. 19 Relative percentage contributions to the Hirshfeld surface area of various intermolecular contacts in compounds 1–4

the methoxy substitution in compound **3** reduces the proportion of H...S hydrogen-bond interactions slightly. The C...H/H...C intermolecular interactions, which represent C–H... π interactions, account for 27.4, 27.1, 24.6, and 28.8 % of the total Hirshfeld surfaces for compounds **1–4**, respectively (Fig. 19). The methyl substitution in compound **4** increases the proportion of C...H hydrogen-bond interactions slightly.

Conclusions

Four novel benzamide derivative compounds were synthesized and characterized by FT-IR, ^1H NMR and ^{13}C NMR spectroscopy techniques. Single-crystal X-ray diffraction was used to characterize all compounds, and detailed study of their crystalline arrangements in solid state was performed. The crystalline and molecular structures of the synthesized compounds **1–4** were examined to determine the effect of the substituent on molecular self-assembly and dimeric synthons and highlight the significance of thiourea derivative compounds in crystal engineering. The packing arrangements of the synthesized compounds were found to be different. Compounds **2** and **3** showed an ideal conformation around the central thiourea moiety for the formation of a dimeric hydrogen-bonded homosynthon (H–N...C=S) as the building block. These dimeric synthons were observed regardless of the formation of different three-dimensional supramolecular networks depending on

different substituents. In these compounds, revealing a significant influence of substituents, a series of dimerization occurs through formation of the consecutive $R_2^2(8)$, $R_2^2(12)$, $R_2^2(14)$, and $R_2^2(28)$ for compound **2** and $R_2^2(18)$ and $R_2^2(28)$ homosynthons for compound **3**. For compounds **1** and **4**, such consecutive synthons were not observed. In addition, the substituents, for example, chloro in case of compound **2**, methoxy in case of compound **3**, and methyl in case of compound **4**, directly participate in formation of noncovalent interactions. Therefore, their electronic influence in directing the formation of 3D structures cannot be ignored. Similarities and differences in intermolecular contacts between compounds were also visualized using Hirshfeld surface analysis. In compounds **1**, **3**, and **4**, the intermolecular H...H contacts contributed more to the crystal packing compared with other interactions. The corresponding contact was found to make a smaller contribution ($\sim 10\%$) in the case of compound **2**. The reduction of H...H contacts is due to the effect of the chlorine substituent at *para* position on the phenyl ring, which reduced intermolecular H...H contacts and was compensated by the presence of H...Cl contacts.

Acknowledgements This work was supported by the Mersin University Research Fund (Project No. 2016-AP4-1426). This academic work was supported linguistically by the Mersin Technology Transfer Office Academic Writing Center of Mersin University.

Authors contribution All authors contributed equally to this work.

Compliance with ethical standards

Conflict of interest The authors declare that they have no conflicts of interest.

Ethical approval All ethical guidelines were adhered to.

Sample availability Samples of the compounds are available from the author.




References

1. R. Custelcean, Chem. Commun. **2008**, 295 (2008)
2. M. Obrzud, M. Rospenk, A. Koll, Phys. Chem. Chem. Phys. **16**, 3209 (2017)
3. U. Solmaz, I. Gumus, G. Binzet, O. Celik, G.K. Balci, A. Dogen, H. Arslan, J. Coord. Chem. **71**(2), 200 (2018)
4. A. Saeed, U. Florke, Acta Crystallogr. E **63**, o3695 (2007)
5. A. Saeed, M.F. Erben, U. Florke, J. Mol. Struct. **982**, 91 (2010)
6. A. Saeed, U. Florke, M.F. Erben, J. Sulfur Chem. **45**, 318 (2014)
7. M.G. Woldu, J. Dillen, Theor. Chem. Acc. **121**, 71 (2008)
8. A. Saeed, R. Qamar, T.A. Fattah, U. Florke, M.F. Erben, Res. Chem. Intermed. **43**, 3053 (2017)
9. A. Saeed, M.F. Erben, U. Shaheen, U. Florke, J. Mol. Struct. **1000**, 49 (2011)
10. J. Guang, A.J. Larson, J.C.G. Zhao, Adv. Synth. Catal. **357**, 523 (2015)
11. Z. Mao, A. Lin, Y. Shi, H. Mao, W. Li, Y. Cheng, C. Zhu, J. Org. Chem. **78**, 10233 (2013)

12. Q. Liu, B. Qiao, K.F. Chin, C.H. Tan, Z. Jiang, *Adv. Synth. Catal.* **356**, 3777 (2014)
13. R.D. Lopez, M.E. Lopez, A. Alcaine, P. Merino, R.P. Herrera, *Org. Biomol. Chem.* **12**, 4503 (2014)
14. W.M. Khairul, A.I. Daud, N.A.M. Hanifaah, S. Arshad, I.A. Razak, H.M. Zuki, M.F. Erben, *J. Mol. Struct.* **1139**, 353 (2017)
15. L. Qiao, J. Huang, W. Hu, Y. Zhang, J. Guo, W. Cao, K. Miao, B. Qin, J. Song, *J. Mol. Struct.* **1139**, 149 (2017)
16. A. Saeed, U. Florke, M.F. Erben, *J. Sulfur Chem.* **35**, 318 (2014)
17. R.S. Correa, K.M.D. Oliveira, F.G. Delolo, A. Alvarez, R. Mocelo, A.M. Plutin, M.R. Cominetti, E.E. Castellano, A.A. Batista, *J. Inorg. Biochem.* **150**, 63 (2015)
18. A.F. Elhousseiny, A. Eldissouky, A.M. Al-Hamza, H.H.A.M. Hassan, *J. Mol. Struct.* **1100**, 530 (2015)
19. N. Selvakumaran, A. Pratheekumar, S.W. Ng, E.R.T. Tiekink, R. Karvembu, *Inorg. Chim. Acta* **404**, 82 (2013)
20. H. Mandal, D. Ray, *Inorg. Chim. Acta* **414**, 127 (2014)
21. V.B. Bregovic, N. Basaric, *Coord. Chem. Rev.* **295**, 80 (2015)
22. Y.M. Zhang, J.D. Qin, Q. Lin, T.B. Wei, *J. Fluor. Chem.* **38**, 1222 (2006)
23. D.H. Lee, H.Y. Lee, K.H. Lee, J. Hong, *Chem. Commun.* **32**, 1188 (2001)
24. J.L. Wu, Y.B. He, Z.Y. Zeng, L.H. Wei, L.Z. Meng, T.Z. Yang, *Tetrahedron* **60**, 4309 (2004)
25. L. Nie, Z. Li, J. Han, X. Zhang, R. Yang, W.X. Liu, F.Y. Wu, J.W. Xie, Y.F. Zhao, Y.B. Jiang, *J. Org. Chem.* **69**, 6449 (2004)
26. G. Binzet, I. Gumus, A. Dogen, U. Flörke, N. Kulcu, H. Arslan, *J. Mol. Struct.* **1161**, 519 (2018)
27. A. Okuniewski, J. Chojnacki, B. Becker, *Acta Crystallogr. E* **68**, 619 (2012)
28. H. Perez, R.S. Correa, A.M. Plutin, B. O'Reilly, M.B. Andrade, *Acta Crystallogr. C* **68**, 19 (2012)
29. L.R. Gomes, L.M.N.B.F. Santos, J.A.P. Coutinho, B. Schroder, J.N. Low, *Acta Crystallogr. E* **66**, 870 (2010)
30. A. Saeed, U. Florke, M.F. Erben, *J. Sulfur Chem.* **35**, 318 (2014)
31. R.R. Cairo, A.M.P. Stevens, T.D. Oliveira, A.A. Batista, E.E. Castellano, J. Duque, D.B. Soria, A.C. Fantoni, R.S. Correa, M.F. Erben, *Spectrochim. Acta A* **176**, 8 (2017)
32. A. Saeed, M. Bolte, M.F. Erben, H. Pérez, *CrystEngComm* **17**, 7551 (2015)
33. A. Saeed, S. Ashraf, U. Florke, Z.Y.D. Espinoza, M.F. Erben, H. Pérez, *J. Mol. Struct.* **1111**, 76 (2016)
34. E.C. Aguilar, G.A. Echeverría, O.E. Piro, S.E. Ulic, J.L. Jios, M.E. Tuttolomondo, H. Pérez, *Mol. Phys.* **116**, 399 (2018)
35. O.V. Dolomanov, L.J. Bourhis, R.J. Gildea, J.A.K. Howard, H. Puschmann, *J. Appl. Cryst.* **42**, 339 (2009)
36. L. Palatinus, G. Chapuis, *J. Appl. Cryst.* **40**, 786 (2007)
37. L. Palatinus, A. van der Lee, *J. Appl. Cryst.* **41**, 975 (2008)
38. L. Palatinus, S.J. Prathapa, S. van Smaalen, *J. Appl. Cryst.* **45**, 575 (2012)
39. G.M. Sheldrick, *Acta Cryst. C* **71**, 3 (2015)
40. A. Linden, *Spec. Acta Cryst. C* **71**, 9 (2015)
41. M.J. Turner, J.J. McKinnon, S.K. Wolff, D.J. Grimwood, P.R. Spackman, D. Jayatilaka, M.A. Spackman, *Crystal Explorer 17* (University of Western Australia, Crawley, 2017)
42. D.S. Mansuroglu, H. Arslan, U. Florke, N. Kulcu, *J. Coord. Chem.* **61**, 3134 (2008)
43. G. Avsar, H. Arslan, H.J. Haupt, N. Kulcu, *Turk. J. Chem.* **27**, 281 (2003)
44. H. Arslan, U. Florke, N. Kulcu, *Acta Chim. Slov.* **51**, 787 (2004)
45. M. Oki, *Top. Stereochem.* **14**, 1 (1983)
46. M. Gemili, H. Sari, M. Ulger, E. Sahin, Y. Nural, *Inorg. Chem. Acta.* **463**, 88 (2017)
47. R. Quintanilla-Licea, J.F. Colunga-Valladares, A. Caballero-Quintero, C. Rodriguez-Padilla, R.T. Guerra, R. Gomez-Flores, N. Waksman, *Molecules* **7**, 662 (2002)
48. A. Rotondo, S. Barresi, M. Cusumano, E. Rotondo, *Polyhedron* **45**, 23 (2012)
49. A. Rotondo, S. Barresi, M. Cusumano, E. Rotondo, P. Donato, L. Mondello, *Inorg. Chim. Acta* **410**, 1 (2014)
50. K.R. Koch, *Coord. Chem. Rev.* **216–217**, 473 (2001)
51. C.K. Ozer, H. Arslan, D. VanDerveer, G. Binzet, *J. Coord. Chem.* **62**, 266 (2009)
52. I.V. Rubtsov, K. Kumar, R.M. Hochstrasser, *Chem. Phys. Lett.* **402**, 439 (2005)
53. H.M. Abosadiya, E.H. Anouar, S.A. Hasbullah, B.M. Yamin, *Spectrochim. Acta A* **144**, 115 (2015)
54. C.G. Overberger, H.A. Friedman, *J. Polym. Sci. A* **3**, 3625 (1965)
55. L. Qiao, Y. Zhang, W. Hu, J. Guo, W. Cao, Z. Ding, Z. Guo, A. Fan, J. Song, J. Huang, *J. Mol. Struct.* **1141**, 309 (2017)

56. Z. Weiqun, L. Baolong, Z. Liming, D. Jiangang, Z. Yong, L. Lude, Y. Xujie, *J. Mol. Struct.* **690**, 145 (2004)
57. C.G. Overberger, H.A. Friedman, *J. Polym. Sci. A* **3**, 3625 (1965)
58. A. Saeed, M.F. Erben, N. Abbas, U. Florke, *J. Mol. Struct.* **984**, 240 (2010)
59. C.N.R. Rao, R. Venkataraghavan, *Spectrochim. Acta A* **18**, 541 (1962)
60. A. Saeed, M.F. Erben, N. Abbas, U. Florke, *J. Mol. Struct.* **984**, 240 (2010)
61. M.S.M. Yusof, R.H. Jusoh, W.M. Khairul, B.M. Yamin, *J. Mol. Struct.* **975**, 280 (2010)
62. A. Saeed, M.F. Erben, M. Bolte, *Spectrochim. Acta A* **102**, 408 (2013)
63. M.F.M. Nasir, I.N. Hassan, W.R.W. Daud, B.M. Yamin, M.B. Kassim, *Acta Crystallogr. E* **67**, o1987 (2011)
64. M.F.M. Nasir, I.N. Hassan, B.M. Yamin, W.R.W. Daud, M.B. Kassim, *Acta Crystallogr. E* **67**, o1742 (2011)
65. N. Gunasekaran, R. Karvembu, S.W. Ngb, E.R.T. Tiekink, *Acta Crystallogr. E* **66**, o2572 (2010)
66. Y. Nural, M. Gemili, N. Seferoglu, E. Sahin, M. Ulger, H. Sari, *J. Mol. Struct.* **1160**, 315 (2018)
67. A. Saeed, A. Khurshid, M. Bolte, A.C. Fantoni, M.F. Erben, *Spectrochim. Acta A* **143**, 59 (2015)
68. H.M. Abosadiya, E.H. Anouar, S.A. Hasbullah, B.M. Yamin, *Spectrochim. Acta A* **92**, 1386 (2015)
69. S. Subhankar, R. Lalit, J. Sumy, M.K. Manish, G. Somnath, R.D. Gautam, *CrystEngComm* **17**, 1273 (2015)
70. M.A. Spackman, D. Jayatilaka, *CrystEngComm* **11**, 19 (2009)
71. M.A. Spackman, J.J. McKinnon, *CrystEngComm* **4**, 378 (2002)
72. A.D. Santo, G.A. Echeverría, O.E. Piro, H. Pérez, A.B. Altabel, D.M. Gil, *J. Mol. Struct.* **1134**, 492 (2017)
73. J.J. McKinnon, M.A. Spackman, A.S. Mitchell, *Acta Crystallogr. B* **60**, 627 (2004)
74. A. Saeed, S. Ashraf, U. Florke, Z.Y.D. Espinoza, M.F. Erben, H. Perez, *J. Mol. Struct.* **1111**, 76 (2016)
75. S.K. Seth, D. Sarkar, A. Roy, T. Kar, *CrystEngComm* **13**, 6728 (2011)
76. I. Gumus, U. Solmaz, S. Gonca, H. Arslan, *Eur. J. Chem.* **8**(4), 349 (2017)
77. I. Gumus, S. Gonca, B. Arslan, E. Keskin, U. Solmaz, H. Arslan, *Eur. J. Chem.* **8**(4), 410 (2017)
78. I. Gumus, U. Solmaz, O. Celik, G. Binzet, G. Balci, H. Arslan, *Eur. J. Chem.* **6**(3), 237 (2015)
79. A. Saeed, R. Qamar, T.A. Fattah, U. Flörke, M.F. Erben, *Res. Chem. Intermed.* **43**(5), 3053 (2017)

Affiliations

Ilkay Gumus¹  · Ummuhan Solmaz¹  · Gun Binzet³  · Ebru Keskin²  ·
Birdal Arslan¹  · Hakan Arslan¹ 

✉ Ilkay Gumus
ilkay.gumus@mersin.edu.tr

Ummuhan Solmaz
ummuhansolmaz@mersin.edu.tr

Gun Binzet
gunbinzet@mersin.edu.tr

Ebru Keskin
ebruuvacin@mersin.edu.tr

Birdal Arslan
birdal.arslan@mersin.edu.tr

Hakan Arslan
hakan.arslan@mersin.edu.tr

- ¹ Department of Chemistry, Faculty of Arts and Science, Mersin University, 33343 Mersin, Turkey
- ² Advanced Technology Research and Application Center, Mersin University, 33343 Mersin, Turkey
- ³ Department of Chemistry, Faculty of Education, Mersin University, 33343 Mersin, Turkey